Undoubtedly the orbital is strongly modified by rehybridization either by removal of an electron from the orbital or by coordination to a Lewis acid. When the carbon lone pair loses an electron or becomes engaged in bonding, it acquires more p character, and the opposite carbon σ orbital (4σ, which is involved in the C-O σ bond) acquires more s character. This increase in s character increases the strength of the C-O bond. Theoretical work of Sherwood and Hall[23] has shown that, even in long-distance interactions of CO with a transition metal, σ rehybridization occurs, with a shift of the lone pair electron density toward the metal and a shortening of the C-O bond.

In the case of BH_3·CO, the extent to which the C-O bond is strengthened by such rehybridization cannot be simply determined from measures of the C-O bond strength (such as the C-O stretching frequency) because π back-bonding causes a simultaneous *weakening* of the bond. However, the situation is simpler in the case of the methyl isocyanide adduct of borane, BH_3·CN-CH_3, because there is little π back-bonding in this molecule. The marked increase in the C-N stretching frequency of 150 cm^{-1} on going from CH_3NC to the adduct[22] must be due entirely to rehybridization of the σ N-C-B system. This conclusion is supported by an ab initio study of CH_3NC that shows that the HOMO has bonding character.[24]

Experimental Section

Diborane was prepared by the reaction of $NaBH_4$ and H_3PO_4.[25] Methyl isocyanide was prepared by the dehydration of *N*-methylformamide.[26] The borane-methyl isocyanide adduct[22] is relatively nonvolatile and was found to form higher oligomers when heated. In order to obtain an adequate flow of vapor into the spectrometer gas cell, the compound was prepared in a 2-l bulb attached to a 2.5-cm valve that led directly to the spectrometer inlet system. Excess methyl isocyanide was condensed over most of the interior surface of the bulb by slowly raising a liquid-nitrogen-filled Dewar around the bulb as the methyl isocyanide was admitted. Diborane was condensed in the flask, and it was allowed to warm to room temperature. The volatile residue was pumped off, leaving the adduct. Sufficient vapor evolved from the solid distributed over this large surface area to obtain spectra at room temperature. The infrared spectrum of the solid in the sample flask agreed with that in the literature.[22]

Borane-phosphorus trifluoride was prepared by the method of Parry and Bissot,[27] in which B_2H_6 is reacted with excess PF_3 (8 atm) for 3 days. The product was purified by fractional condensation, and its vapor pressure (23 mm at -111.8 °C) agreed with that in the literature. To minimize the dissociation of BH_3·PF_3, the sample was stored at -196 °C, fractionated immediately prior to use, and held at -111.8 °C during the collection of spectra. The B_2H_6 B 1s peak is separated from the B 1s peak of the adduct by more than 2 eV and was not observed. The measured phosphorus and fluorine binding energies of BH_3·PF_3 are very similar to those of PF_3, so that free PF_3 would not be readily observed. The absence of a peak attributable to diborane is our principal evidence that the compound does not dissociate under the conditions of measurement.

Borane-ammonia was obtained commercially (Alfa) and was sublimed before use. The spectrometer was heated to 50 °C, at which temperature a very weak signal was obtained. Attempts to use higher temperatures resulted in decomposition. The half-widths of the B 1s and N 1s lines were unusually broad, probably because of spectrometer drift during the 20 h necessary to obtain the spectra, even though a drift correction was applied every 30 min.

Gas-phase X-ray photoelectron spectra were obtained with a GCA/McPherson ESCA 36 spectrometer utilizing a Mg anode. Nitrogen gas served as the internal calibrant, and the Ne 1s, N_2 1s, and Ne 2s photolines were used to determine the linearity of the spectrometer. Procedural details have been described elsewhere.[28]

Acknowledgment. This work was supported by the Director, Office of Energy Research, Office of Basic Energy Sciences, Chemical Sciences Division of the U.S. Department of Energy under Contract No. DE-A003-76SF00098.

Registry No. BH_3·NH_3, 13774-81-7; BH_3·$N(CH_3)_3$, 75-22-9; BH_3·CO, 13205-44-2; BH_3·$CNCH_3$, 62630-46-0; BH_3·PF_3, 14931-39-6; BH_3·$P(CH_3)_3$, 1898-77-7.

(23) Sherwood, D. E.; Hall, M. B. *Inorg. Chem.* **1983**, *22*, 93.
(24) Bevan, J. W.; Sandorfy, C.; Pang, F.; Boggs, J. E. *Spectrochim. Acta, Part A* **1981**, *37A*, 601.
(25) Norman, A. D.; Jolly, W. L. *Inorg. Synth.* **1968**, *11*, 15.
(26) Cassanova, J. C.; Parry, R. W. *J. Am. Chem. Soc.* **1963**, *85*, 4280.
(27) Parry, R. W.; Bissot, T. C. *J. Am. Chem. Soc.* **1956**, *78*, 1524.
(28) Chen, H. W.; Jolly, W. L.; Kopf, J.; Lee, T. H. *J. Am. Chem. Soc.* **1979**, *101*, 2607.

Contribution from the Istituto di Chimica Generale ed Inorganica, University of Padova, 35100 Padova, Italy, and Istituto di Chimica Generale ed Inorganica, University of Torino, Torino, Italy

UV Photoelectron and Theoretical Studies of Organometal Carbonyl Clusters of Ruthenium and Osmium. μ-Hydrido-μ_3-Allyl and μ-Hydrido-μ_3-Allenyl Triangulo Cluster Compounds

GAETANO GRANOZZI,*[1a] EUGENIO TONDELLO,[1a] RENZO BERTONCELLO,[1a] SILVIO AIME,[1b] and DOMENICO OSELLA[1b]

Received March 21, 1984

The electronic structures of μ-hydrido-μ_3-allyl and μ-hydrido-μ_3-allenyl triangulo clusters of ruthenium and osmium are discussed on the basis of both He I and He II gas-phase UV-PE spectra and CNDO quantum-mechanical calculations. The theoretical results contribute to the discussion of the PE data and to a deeper understanding of the bonding scheme in these very complex organometallic clusters. The description of the allyl cluster interactions in terms of one π and two σ bonds seems to be adequate. On the other hand, the formal distinction into one σ and two π bonds of the allenyl ligand cluster interaction is quite an oversimplification of the actual bonding scheme. The differences in thermodynamical stability between the allenyl and allyl derivatives are in agreement with the CNDO-computed total energies.

Introduction

It is now well established that many reactions involving $M_3(CO)_{12}$ clusters (M = Ru, Os) often afford hydrido-organometal clusters by oxidative addition of the incoming ligand.[2] In particular, in the thermal reactions of $M_3(CO)_{12}$ with alkynes (L-H) (contg. a hydrogen atom on the carbon in α position to the unsaturated sites) two isomeric compounds of formula $HM_3(CO)_9(L)$ are usually formed in good or moderate yields.[3-6]

(1) (a) University of Padova. (b) University of Torino.
(2) Johnson, B. F. G.; Lewis, J. *Adv. Inorg. Chem. Radiochem.* **1981**, *24*, 225.
(3) Gambino, O.; Valle, M.; Aime, S.; Vaglio, G. A. *Inorg. Chim. Acta* **1974**, *8*, 71.
(4) Aime, S.; Milone, L.; Osella, D.; Valle, M. *J. Chem. Res. Synop.* **1978**, *77*; *J. Chem. Res., Miniprint* **1978**, *77*, 785-797.
(5) Ferrari, R. P.; Vaglio, G. A. *J. Organomet. Chem.* **1979**, *182*, 245.
(6) Ferrari, R. P.; Vaglio, G. A. *Gazz. Chim. Ital.* **1975**, *105*, 939.

0020-1669/85/1324-0570$01.50/0

Table I. Ionization Energy Data (eV) for the Studied Organometal Carbonyl Clusters[a]

1a	1b	1c	2a	2b
7.81 (A + B)	7.82 (A + B)	8.00 (A)	7.90 (A)	7.82 (A)
		8.30 (B)	8.13 (B)	8.23 (B)
8.95 (C)	9.02 (C)	9.31 (C)	9.09 (C + D)	9.18 (C)
9.39 (D)	9.36 (D)	9.58 (D)		9.57 (D)
		9.86 (D')		
10.10 (E + F)	10.08 (E + F)	10.57 (E)	10.34 (E + F)	10.33 (E)
		10.95 (F)		10.66 (F)
				10.89 (F')
10.81 (G)	10.95 (G)	11.52 (G)	11.47 (G + H)	11.71 (G)
11.70 (H + J)	11.57 (H)	12.30 (H + J)		12.11 (H)
	12.00 (J)		12.19 (J)	12.47 (J)

[a] Band labels are in parentheses.

Isomer **2** (containing a 1-η^1-1,2-η^2-allenyl ligand)[7] is the kinetically favored isomer whereas isomer **1** (containing a 1,3-

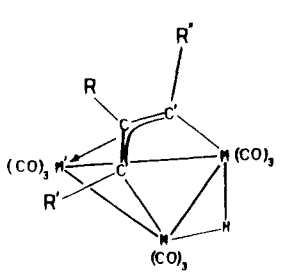

1

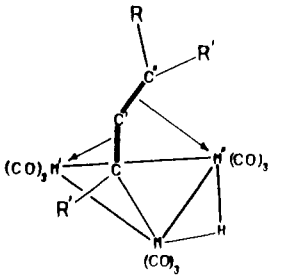

2

η^1-η^3-allyl ligand)[8] is the thermodynamically stable one. The isomerization process **2** → **1** (which occurs through both thermal and photochemical activation) does not take place by simple hydrogen atom migration in the organic framework, but it has been found that an intramolecular exchange between the allenic H and the hydridic H is occurring in **2** before a detectable isomerization could have been observed.[9] A number of studies have already been devoted to these isomers by different experimental approaches. NMR spectroscopy has shown[10,11] that a localized CO exchange at each $M(CO)_3$ unit is occurring in both types of complexes, but in **2** it has also been shown that an edge-hopping of the hydride ligand and a simultaneous "wagging" motion of the organic ligand are occurring in the range of the reported temperatures; on the other hand, in **1** no motion of the allyl ligand can be detected on the NMR time scale.

A preliminary investigation[12] on the ruthenium **1** and **2** derivatives suggested that these systems, in contrast to the parent carbonyl $Ru_3(CO)_{12}$, do not undergo a photodeclusterification. Actually, a coordinatively unsaturated species, formed by loss of a CO ligand, is obtained under photochemical irradiation of **1**.

In order to get a better understanding of the electronic structures of these organometal carbonyl clusters and as a development of our previous studies on the electronic structures of related carbonyl clusters,[13-20] we have recorded the gas-phase UV photoelectron spectra of examples of isomers of **1** and **2** (M = Ru, Os). The PE data will be discussed also on the basis of the results of quantum-mechanical calculations. Since the complexity of the studied molecules prevents the use of nonempirical ab initio methods, we decided to adopt the CNDO semiempirical scheme whose results for similar molecules showed a satisfactory agreement with the PE data.[13-18,20] Furthermore, the theoretical results will assist us in drawing a picture of the bonding schemes in such compounds.

Experimental Section

The compounds $HRu_3(CO)_9(MeC{=}CH{=}CMe)$ (**1a**), $HRu_3(CO)_9(HC{=}CH{=}CMe)$ (**1b**), $HOs_3(CO)_9(HC{=}CH{=}CMe)$ (**1c**), $HRu_3(CO)_9(MeC{=}C{=}CMe_2)$ (**2a**), and $HOs_3(CO)_9(MeC{=}C{=}CMe_2)$ (**2b**) were prepared by the reaction of $M_3(CO)_{12}$ (M = Ru, Os) and the appropriate olefin or alkyne as described in detail elsewhere.[3,4,6,21,22] It is proper to observe here that, in order to avoid the thermal isomerization process **2** → **1** in the ionization chamber of the PE spectrometer, the allenic hydrogen atom has been replaced by a methyl group in both **2a** and **2b** compounds.

He I and He II excited PE spectra were measured on a Perkin-Elmer PS-18 spectrometer modified for He II measurements by inclusion of a hollow cathode discharge lamp that gives a high photon flux at He II wavelengths (Helectros Developments). The ionization energy (IE) scale was calibrated by reference to peaks due to admixed inert gases (Xe–Ar) and to the He self-ionization. The IEs reported in Table I are the mean values over several distinct runs. A heated inlet probe in the 60–100 °C temperature range was used.

Quantum-mechanical calculations were performed by a version of the CNDO method[23] suitable for transition-metal complexes. Ru semiempirical parameters were obtained[23] from atomic spectroscopical data whereas the C, O, and H parameters are Pople's standard ones.[24] Gross atomic charges and bond overlap populations were obtained by Mulliken's population analysis[25] of the deorthogonalized[26] eigenvectors. The geometrical parameters used in the calculations were taken from the X-ray structural determinations.[7,8]

PE Results

The low-IE regions (up to 13 eV) of the PE spectra of several **1** and **2** type compounds are shown in Figures 1 and 2. Table I lists the vertical IE values for these clusters.

A common feature of the PE spectra of the studied clusters (and in general of carbonyl clusters) is the presence of a broad and poorly resolved band beyond 13.5 eV due to carbonyl 5σ and 1π ionizations. This broad band prevents the detection in this region of resolved peaks. This is the reason why we have reported the lower IE region.

(7) Gervasio, G.; Osella, D.; Valle, M. *Inorg. Chem.* **1976**, *15*, 1221.
(8) Evans, M.; Hursthouse, M.; Randall, E. W.; Rosenberg, E.; Milone, L.; Valle, M. *J. Chem. Soc., Chem. Commun.* **1972**, 545.
(9) Aime, S.; Osella, D.; Milone, L.; Rosenberg, E., manuscript in preparation.
(10) Aime, S.; Milone, L.; Osella, D.; Valle, M.; Randall, E. W. *Inorg. Chim. Acta* **1976**, *20*, 217.
(11) Aime, S.; Gobetto, R.; Osella, D.; Milone, L.; Rosenberg, E. *Organometallics* **1982**, *1*, 640.
(12) Amadelli, R.; Carassiti, V.; Maldotti, A.; Aime, S.; Osella, D.; Milone, L. *Inorg. Chim. Acta* **1984**, *81*, L11.
(13) Granozzi, G.; Tondello, E.; Bertoncello, R.; Aime, S.; Osella, D. *Inorg. Chem.* **1983**, *22*, 744.
(14) Ajo', D.; Granozzi, G.; Tondello, E.; Fragala', I. *Inorg. Chim. Acta* **1979**, *37*, 191.
(15) Granozzi, G.; Tondello, E.; Benard, M.; Fragala', I. *J. Organomet. Chem.* **1980**, *194*, 83.
(16) Granozzi, G.; Tondello, E.; Casarin, M.; Ajo', D. *Inorg. Chim. Acta* **1981**, *48*, 73.
(17) Granozzi, G.; Tondello, E.; Ajo', D.; Casarin, M.; Aime, S.; Osella, D. *Inorg. Chem.* **1982**, *21*, 1081.
(18) Granozzi, G.; Benoni, R.; Acampora, M.; Aime, S.; Osella, D. *Inorg. Chim. Acta* **1984**, *84*, 95.
(19) Granozzi, G.; Benoni, R.; Tondello, E.; Casarin, M.; Aime, S.; Osella, D. *Inorg. Chem.* **1983**, *22*, 3899.
(20) Granozzi, G.; Bertoncello, R.; Aime, S.; Osella, D. *J. Organomet. Chem.* **1982**, *229*, C27.
(21) Rosenberg, E.; Aime, S.; Milone, L.; Sappa, E.; Tiripicchio, A.; Manotti Lanfredi, A. M. *J. Chem. Soc., Dalton Trans.* **1981**, 2023.
(22) Deeming, A. J.; Hasso, F.; Underhill, M. *J. Chem. Soc., Dalton Trans.* **1975**, 1614.
(23) Tondello, E. *Inorg. Chim. Acta* **1974**, *11*, L5.
(24) Pople, J. A.; Segal, G. A. *J. Chem. Phys.* **1966**, *44*, 3289.
(25) Mulliken, R. S. *J. Chem. Phys.* **1955**, *23*, 1833.
(26) Löwdin, P. O. *J. Chem. Phys.* **1950**, *18*, 365.

Table II. CNDO Results for $HRu_3(CO)_9(MeC{=}CH{=}CMe)$

		% population							
		Ru							
MO	eigenvalue, eV	2 Ru	Ru′	H	CH	2 C′	9 CO	$2\,CH_3$	dom char
32a″	−7.14	45	23	0	1	17	9	5	Ru–Ru′ bonds
39a′	−7.22	47	35	0	2	2	14	0	
38a′	−8.97	60	23	1	2	0	14	0	4d metal-based MOs mainly maintaining atomlike character (nonbonding)
31a″	−9.10	80	6	0	1	1	10	2	
30a″	−9.29	77	14	0	0	0	9	0	
37a′	−9.29	58	28	0	2	1	11	0	
29a″	−9.44	69	13	0	2	3	12	1	
36a′	−9.53	5	79	0	0	0	16	0	
35a′	−9.57	86	1	0	2	0	10	1	
28a″	−9.68	30	52	0	0	6	11	1	
34a′	−10.11	58	26	2	0	0	14	0	
33a′	−10.27	47	15	20	1	1	15	1	Ru–H–Ru bond
32a′	−11.61	24	7	11	8	31	13	6	ligand cluster bonds
27a″	−12.23	25	2	0	7	36	18	12	
31a′	−13.71	5	6	0	29	16	15	29	

Table III. CNDO Results for $HRu_3(CO)_9(MeC{=}C{=}CHMe)$

		% population										
		Ru										
MO	eigenvalue, eV	Ru	Ru′	Ru″	H	C′	C	C″H	CH_3	CH_3′	9 CO	dom char
71a	−6.94	30	32	20	0	2	1	1	0	1	13	Ru–Ru′, Ru′–Ru″ bonds
70a	−7.18	21	34	30	0	1	4	3	0	0	7	
69a	−8.54	50	8	11	2	5	6	8	1	1	8	4d metal-based MOs mainly maintaining atomlike character (nonbonding)
68a	−8.90	44	37	9	2	0	1	0	0	0	7	
67a	−9.01	23	43	21	0	0	0	0	0	0	13	
66a	−9.06	27	42	18	0	0	1	0	0	0	12	
65a	−9.22	59	2	24	0	0	1	0	0	1	13	
64a	−9.30	2	22	61	0	1	0	0	0	0	14	
63a	−9.33	11	41	29	1	1	3	1	0	1	13	
62a	−9.64	1	24	57	0	1	1	5	3	0	8	
61a	−9.87	22	20	41	3	0	1	1	0	0	12	
60a	−10.03	31	9	23	18	1	2	2	0	0	14	Ru–H–Ru″ bond
59a	−10.53	27	15	7	1	4	17	12	4	6	7	ligand cluster bonds
58a	−12.70	6	9	4	1	22	20	12	10	11	5	
57a	−14.04	3	1	5	0	19	16	9	13	22	12	

By analogy to PE data collected for other trimetallic clusters of Ru and Os,[13,18-20] it is convenient to divide the lower IE region into three parts that correspond to ionizations from MOs with a peculiar predominant character, i.e. metal–metal bonding, metallic "*n*d" nonbonding, and cluster–substrate bonding MOs.

The bands labeled A and B in Figures 1 and 2 can be reasonably assigned to ionizations that essentially represent the M–M bonding levels. These bands are resolved in the cases of **1c**, **2a**, and **2b** derivatives while a symmetric band is present for the **1a** and **1b** ones. Bands C–F are related to ionizations from MOs largely localized on the metal atoms with predominant nonbonding *n*d character, referenced as "t_{2g} like" because of their parentage with pseudo-t_{2g} orbitals of a $M(CO)_4$ fragment. As previously shown,[19,27] the ionizations within the t_{2g} set can be split into several components according to the geometrical arrangement of the metallic framework and the nature of the ligands. Sherwood et al.[27] suggested to divide them in two subsets according to their metal–metal bonding or antibonding character ("t_{2g}^{b}" and "t_{2g}^{a}"), the latter lying at lower IEs. We suggest, in particular, to assign bands E and F, which are present nearly at the same IE in all the trinuclear clusters containing a $M_3(CO)_9$ subunit,[13,18-20] to stabilized in-phase t_{2g}^{b} orbitals. The bands labeled G, H, and J are to be related to M–H–M, M_3–allyl, and –allenyl bonding levels. The He II PE spectrum of **1b** (Figure 1) proves that band G and bands H and J to a larger extent are to be assigned to ionizations from MOs mostly localized in the organic portion of the molecule. In fact, the marked intensity decrease of these bands in the He II spectrum leads us to predict a large participation of C_{2p} and H_{1s} AOs, whose cross sections, on the assumption of the Gelius model,[28] are considerably lower under He II radiation when compared to the *n*d metallic ones.[29]

In the next section, we will first examine the results of CNDO calculations on the studied clusters and then we will discuss the band assignments in more detail.

Discussion

On the basis of the empirical EAN rule, the title compounds can be qualitatively described as 48-electron saturated clusters when the allyl and allenyl ligands are considered as five-electron donors. The allyl ligand is described as bound to the trimetallic cluster through two σ M–C bonds and one π bond, whereas the allenyl ligand is bound through one σ M–C bond and two π bonds. A deeper understanding of the bonding scheme in these organometallic clusters can be accomplished by using some quantum-mechanical tool.

CNDO-computed eigenvalues and eigenvectors of the 15 outermost MOs of **1a** and **2a** derivatives are reported in Tables II and III The CNDO results provide an eigenvalue spectrum (within the Koopmans theorem[30]) that is as a whole in agreement with the reported PE data: in particular the 15 outermost MOs gather into three groups whose order and character correspond to the PE regions assigned on the basis of comparative arguments. Bearing in mind the limitations of the semiempirical approach and the molecular complexity, a one-by-one matching between the theoretical and the experimental PE data is out of reach. For

(27) Sherwood, D. E., Jr.; Hall, M. B. *Inorg. Chem.* **1982**, *21*, 3458.

(28) Gelius, U. In "Electron Spectroscopy"; Shirley, D. A., Ed.; North-Holland Publishing Co.: Amsterdam, 1972; p 311.

(29) Rabalais, J. W. In "Principles of UV Photoelectron Spectroscopy"; Wiley Interscience: New York, 1977.

(30) Koopmans, T. *Physica* **1933**, *1*, 104.

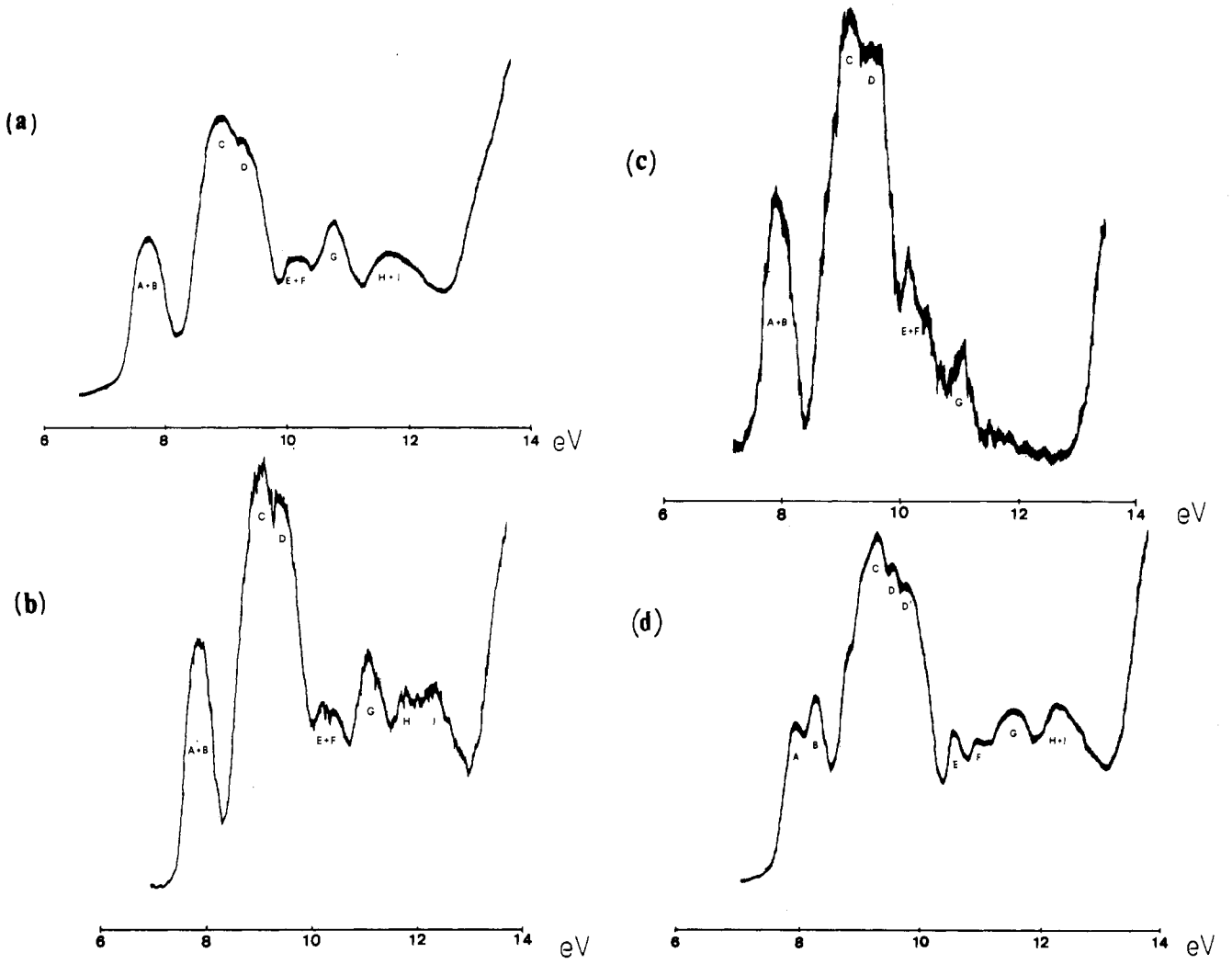

Figure 1. He I excited PE spectra: (a) $HRu_3(CO)_9(MeC{=}CH{=}CMe)$ (**1a**); (b) $HRu_3(CO)_9(HC{=}CH{=}CMe)$ (**1b**); (c) $HRu_3(CO)_9(HC{=}CH{=}CMe)$ (**1b**) (He II spectrum); (d) $HOs_3(CO)_9(HC{=}CH{=}CMe)$ (**1c**).

this reason, during the following discussion, the theoretical results will be used as an aid rather than as a final criterion for the spectral assignments.

$HM_3(CO)_9$–Allyl. The two outmost MOs (32a″, 39a′), which result nearly degenerate from the CNDO calculation, show metal–metal bonding character and are originated from two of the three "e_g-like" M–M bonding MOs of $M_3(CO)_{12}$.[13,14,18,27,31] In particular, the eigenvector analysis of the HOMO reveals a relevant contribution (18% in Table II) from the unoccupied π_2 MO of the allyl fragment:

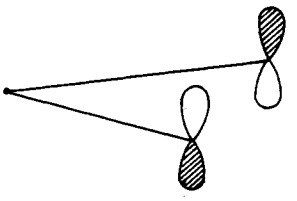

The presence of such a contribution could explain both the degeneracy and the large intensity experimentally found for the band envelope A + B in **1a** and **1b** (Figure 1). As a matter of fact, the interaction between the unoccupied π_2 MO of the allyl ligand and the suitable MO of the trimetallic moiety must be considered as a back-bonding interaction $M_3 \rightarrow$ allyl that results in the shift of the HOMO toward the inner one; moreover, the large He I photoelectron cross sections of the C_{2p} AOs justify the large intensity of band A + B. Such a back-bonding interaction is peculiar to the allyl ligand due to its low-lying π_2 virtual level. Actually, no evidence of such interaction has been found in the outermost MOs for alkynyl cluster derivatives[13] and for the allenyl ones (vide infra) where the two bands A and B are resolved. However, in the osmium derivative **1c**, the lower IE region results in two well-separated A and B components.

The following nine orbitals, largely localized on the metal centers, represent nonbonding MOs maintaining metal d character (with some mixing with carbonyl $2\pi^*$ MOs) and are associated to the t_{2g} bands C, D, and E + F. With respect to $Ru_3(CO)_{12}$,[13,14,31] the C–D splitting is smaller and a shift toward lower IEs is present. These effects probably reflect an orbital mixing with inner ligand orbitals and an overall charge transfer toward the M_3 ring, in tune with the results for the alkynyl derivative.[13] Band E + F, at higher IE and well apart from C and D, is to be related to two t_{2g}^b-stabilized MOs. This assignment is confirmed by the PE spectrum of the Os derivative where the corresponding band is split into two resolved components and by the trend of the band intensities in the He II spectrum of **1b** (Figure 1).

The next four MOs (33a′, 32a′, 27a″, 31a′) are to be related to cluster–substrate and cluster–hydride bonding orbitals. MO 33a′ shows a large contribution of the bridging hydride AO (20%) and of the corresponding two metallic centers (47%). These findings suggest a three-center two-electron M–H–M MO[32,33]

(31) (a) Green, J. C.; Mingos, D. M. P.; Seddon, E. A. *Inorg. Chem.* **1981**, *20*, 2595. (b) Green, J. C.; Seddon, E. A.; Mingos, D. M. P. *J. Chem. Soc., Chem. Commun.* **1979**, 94.

(32) Bau, R.; Teller, R. G.; Kirtley, S. W.; Koetzle, T. F. *Acc. Chem. Res.* **1979**, *12*, 176.

(33) Churchill, M. R.; De Boer, B. G.; Rotella, F. J. *Inorg. Chem.* **1976**, *15*, 1843.

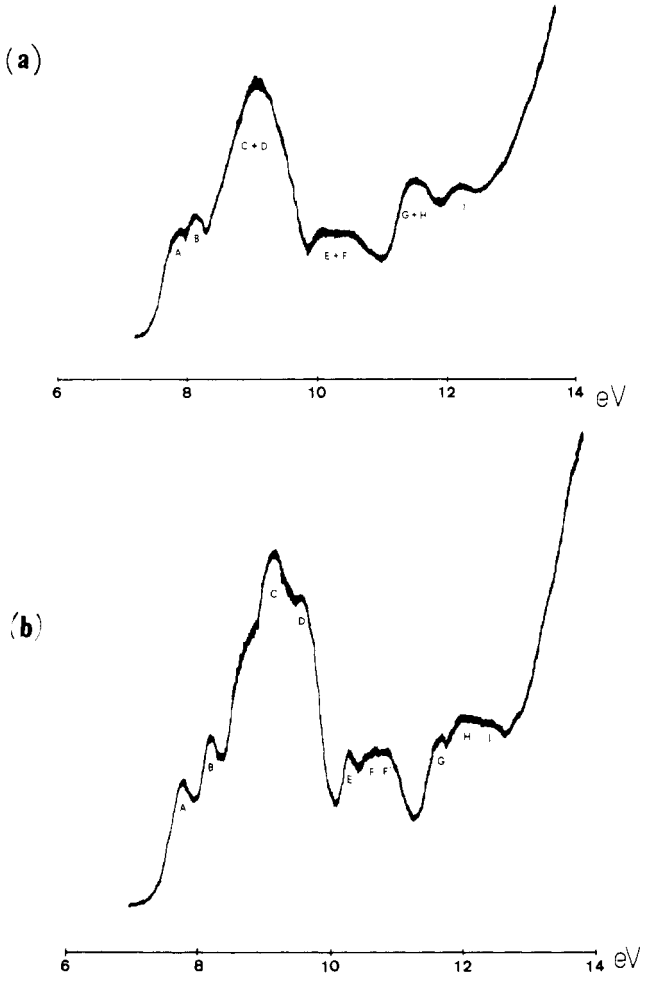

Figure 2. He I excited PE spectra: (a) $HRu_3(CO)_9(MeC{=}C{=}CMe_2)$ (**2a**); (b) $HOs_3(CO)_9(MeC{=}C{=}CMe_2)$ (**2b**).

ideally related to the third M–M bonding MO lacking in the first spectral region, particularly modified and stabilized by the hydride interaction. The next two MOs (32a′, 27a″) are to be related to the metal–allyl ligand σ levels. The corresponding eigenvectors show a large contribution from allyl carbon AOs that are related to in-phase and out-of-phase combinations (n_+ and n_-) of the "radical lobes" of the allyl fragment. From the CNDO calculation performed on the allyl fragment, these n_+ and n_- orbitals represent the LUMO and HOMO of the cationic fragment and the two outermost occupied MOs of the anionic fragment, respectively. As it can be seen in

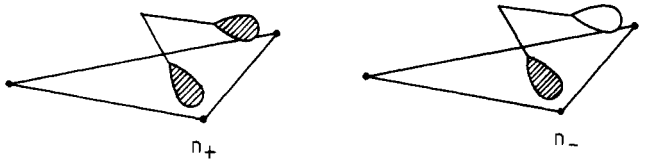

these orbitals point directly toward the two metallic centers and are suitable for cluster–allyl σ interactions. The inner MO (31a′) is particularly localized on the allyl ligand, and the eigenvector analysis shows a π_1 allyl parentage with an in-phase mixing with orbitals of the Ru′ atom.

The theoretical energy sequence of these four MOs does not furnish correct assignments of bands G, H, and J. On the basis of intensity arguments and comparison with literature data,[13-20,27,31] we propose to assign band G to the ionizations from the two metal allyl σ levels (32a′ and 27a″ MOs) whereas bands H and J (split in the asymmetrically substituted allyl ligand **1b** and degenerate in the symmetrical one **1a**) are related to M–H–M and π_1 levels, respectively. The theoretical results confirm the assignment as far as the sequence of σ/π MOs is concerned, but they do not agree with the position of the M–H–M ionization, which is predicted

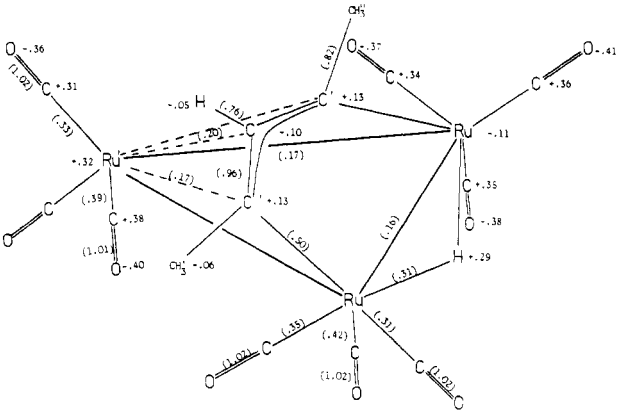

Figure 3. CNDO gross atomic charges and overlap populations (in parentheses) of $HRu_3(CO)_9(MeC{=}CH{=}CMe)$.

at lower IE (Table II). Experimental support to these assignments comes from the analysis of the He II spectrum[34] and from the comparison with the IE values for the M–H–M ionizations in other transition-metal complexes with hydrido bridges (values ranging from 11.0 to 13.5 eV[13,19,27,31]). The experimental shift toward lower IE of band J in the symmetrically substituted allyl derivative **1a** is presumably due to a substituent effect on the highly polarizable π_1 orbital when a hydrogen atom is replaced by a methyl group.

In summary of the body of above data, a bonding picture emerges that is very similar to the qualitative one previously reported. The 32a′ and 27a″ MOs represent the two σ allyl cluster interactions through which the allyl ligand donates charge to the two bridged Ru atoms whereas the π allyl cluster interaction is composed by two opposite contributions: the 32a″ MO describes the back-donation from a M–M′ bonding orbital of the cluster to the π_2 empty allyl orbital while the 31a′ MO is related to the charge donation from the π_1 occupied allyl orbital (mainly from the central carbon atom) to the unique M′ atom.

The Mulliken population analysis of the CNDO eigenvectors reported in Figure 3, is in full agreement with the bonding scheme just described. The comparison between the positive charge of Ru′ with the negative ones of the two equivalent Ru atoms and the corresponding charge differences of the carbon allyl atoms reflects the different existing interactions. In particular, the two Ru atoms are electron rich due to the donation from the allyl ligand and the hydrido bridge whereas the Ru′ one is relieved of charge mainly through the back-bonding mechanism. Accordingly, the two σ Ru–C overlap populations (OPs) are significantly larger than the Ru′–C and Ru′–C′ π ones.[35] It is quite interesting also to compare the OPs relative to the metallic triangle with those previously reported for the related alkynyl derivative.[13] In the present case we note an equivalent reduction of the three Ru–Ru OPs with respect to those of $Ru_3(CO)_{12}$[14] whereas in the alkynyl derivative the bridged Ru–Ru OP was particularly small (0.07 e in ref 13). The charge enrichment of the two Ru centers (σ bonded to the allyl ligand) probably causes their orbital expansion, which allows a better metal–metal interaction. From this point of view the

interaction is a "closed" one[32,33] in contrast with the "open" structure proposed for the alkynyl derivative.[13]

$HM_3(CO)_9$-Allenyl. From the results of the X-ray diffraction analysis[7] it turns out that the qualitative description of the bonding of the allenyl fragment with the metallic triangle in terms of one σ and two π contributions is at least an oversimplification. In

(34) According to literature data,[27,28,31] the M–H–M ionizations suffer the largest intensity decrease under He II radiation because of the very low He II photoionization cross sections of the H 1s AO.

(35) It is proper here to point out that the Ru–C interactions are strictly σ in character because the plane of the allyl ligand contains the two Ru atoms. On the contrary, the Ru′–allyl interaction is not strictly π, but it presents some σ contribution.

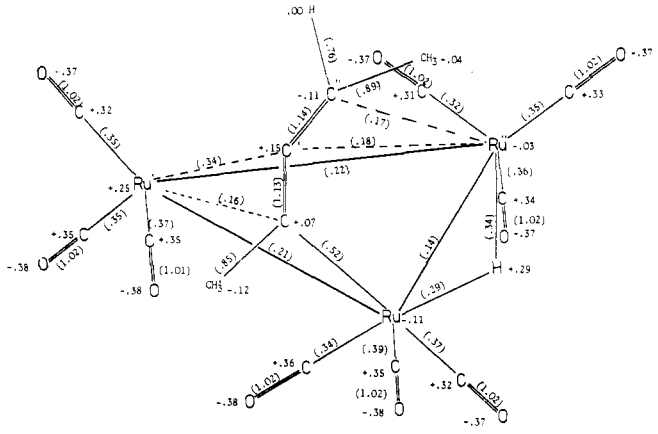

Figure 4. CNDO gross atomic charges and overlap populations (in parentheses) of $HRu_3(CO)_9(MeC{=}C{=}CHMe)$.

fact the Ru–C bond length (2.06 Å), that is the σ bond, is not significantly shorter than the Ru′–C′ one (2.09 Å), which is formally described as a π bond. On the other hand, the lack of molecular symmetry and the marked deformation of the allenyl skeleton (C=C′=C″ angle is $\simeq$142°) make difficult the interpretation of the theoretical results (Table III) in terms of σ and π contributions. Bearing in mind these limitations, we will continue in the following to use the "σ" and "π" notation only for conciseness reasons.

As in the allyl cluster derivative, an overall agreement between the CNDO results (Table III) and the general features of the **2a** and **2b** PE spectra is found. MOs 71a and 70a represent metal–metal bonding levels and are related to bands A and B in the PE spectra of **2a** and **2b**. The eigenvector analysis of these MOs, unlike the corresponding allyl ones, shows no significant contribution from the AOs of the allenyl carbon atoms. The next seven MOs (up to 63a) are unequivocally assigned to *n*d nonbonding levels and correspond to band C + D in the PE spectra of **2a** and **2b**. The following spectral region includes ionizations due to the allenyl cluster interactions. Band E + F, by intensity arguments and by comparison with the spectrum of **2b** where it is split in E, F, and F′, is to be related to three ionizations: two of them correspond to t_{2g}-like-stabilized *n*d levels while the third is assigned to the Ru–C "σ" interaction. 62a, 61a, and 59a MOs represent the CNDO counterpart of these assignments. Consistently with the assignments proposed for the allyl analogues, bands G + H and J are to be related to M–H–M (60a) and to the two metal–ligand "π" interactions (58a, 57a). That the aforementioned σ/π notation is an oversimplification is clearly evident from the populations of 57a, 58a, and 59a MOs (Table III). For example, the 59a MO, which predominantly describes the Ru–C "σ" bond, shows remarkable contributions also from Ru′, Ru″, C′, and C″ atoms. This is at variance with the results obtained for the allyl derivative, where the σ/π contributions were well factored.

Further information about the bonding scheme can be achieved by the Mulliken population analysis (Figure 4). A first interesting remark is the unequivalence among the three ruthenium atoms that show different atomic charges. The atomic charge of Ru, involved both in the "σ" bond with the allenyl ligand and in the M–H–M bond, is equivalent to that of the σ-bonded Ru atoms in the allyl derivative (−0.11 e).

An estimate of the overall bond strength between the allenyl fragment and the metallic framework can be obtained looking at the relative OPs. The Ru–C "σ" and the Ru′–C′ "π" bonds show the major OP values (0.52 and 0.34 e, respectively) while the remainder of the metal–allyl interactions show OP values ranging from 0.16 to 0.18 e. In accordance with previous considerations, these findings correlate with the experimental bond lengths.

Concluding Remarks

The present study addresses the difficult problem of describing the electronic structures of very complex organometal clusters through the combined use of PES and CNDO MO calculations. The consistent theoretical and experimental results obtained allow us to gather the high-lying MOs into three groups with different predominant character, i.e. metal–metal bonding, metallic *n*d nonbonding, and cluster–substrate bonding orbitals. Furthermore, the CNDO results allowed us to verify the qualitative bonding schemes so far adopted to describe the bonding between the metallic triangle and the allyl or allenyl fragments. The description of the allyl cluster interactions in terms of one π and two σ bonds seems to be adequate. In particular, the separation of the π cluster allyl interaction into donation and back-donation contributions has been demonstrated. As far as the allenyl ligand cluster interaction, a detailed analysis of both CNDO and X-rays[7] results suggests a mixing between σ and π contributions for each metal–ligand interaction so that the qualitative picture in terms of one σ and two π bonds is an unacceptable oversimplification.

On the other hand, peculiar theoretical evidence, with no experimental confirmation (nor denial, however), concerns the M–H–M interaction; the overlap population and gross atomic charge values of both the allenyl and allyl derivatives let us suppose a "closed" type[32,33]

interaction. This fact, in contrast with what found in the alkynyl derivative,[13] where a very weak M–M OP is present, agrees with a charge enrichment of the bridged metal atoms due to the interaction with allenyl and allyl ligands.

Further evidence of the CNDO effectiveness results from the calculated total energy values; in fact, the allyl derivative is computed to be more stable than the allenyl one in agreement with the relative isomerization (**2** → **1**) data.

Acknowledgment. Thanks are due to the Ministero della Pubblica Istruzione (Grant MPI 12/2/15), to the CNR of Rome for generous financial support to this study, and to Johnson-Matthey Ltd. for a loan of $RuCl_3$ and OsO_4.

Registry No. **1a**, 56943-13-6; **1b**, 52504-78-6; **1c**, 55073-01-3; **2a**, 80400-37-9; **2b**, 80662-58-4; $HRu_3(CO)_9(MeC{=}C{=}CHMe)$, 56943-14-7.